Inorganic Chemistry

Article

pubs.acs.org/IC

Selenadiazolopyridine: A Synthon for Supramolecular Assembly and Complexes with Metallophilic Interactions

Goutam Mukherjee,[†] Puspendra Singh,[†] Chandrasekhar Ganguri,[†] Sagar Sharma,[†] Harkesh B. Singh,*[,†] Nidhi Goel,[‡] Udai P. Singh,[‡] and Ray J. Butcher[§]

[†]Department of Chemistry, Indian Institute of Technology, Bombay, Mumbai 400076, India

[‡]Department of Chemistry, Indian Institute of Technology, Roorkee 247667, India and

[§]Department of Chemistry, Howard University, Washington, DC 20059, United States

Supporting Information

ABSTRACT: The synthesis and characterization of the complexes of Cu(I), Ag(I), Cu(II), and Co(II) ions with 1,2,5-selenadiazolopyridine (psd) is reported. The following complexes have been prepared: $[Cu_2(psd)_3(CH_3CN)_2]^{2+}2(PF_6^-)$; $[(CuCl)_2(psd)_3]$; $[Cu_2(psd)_6]^{2+}2(ClO_4)^-$; $[Ag_2(psd)_2]^{2+}2(NO_3)^-$; $[Ag_2(psd)_2]^{2+}2(CF_3COO)^-$; $[Cu(psd)_2(H_2O)_3]^{2+}2(ClO_4)^-\cdot(psd)_2$; $[Cu(psd)_4(H_2O)]^{2+}2(ClO_4)^-\cdot(CHCl_3)$; $[Cu(psd)_2(H_2O)_3]^{2+}2(NO_3)^-\cdot(H_2O)\cdot(psd)_2$, and $[Co(psd)_2(H_2O)_4]^{2+}2(ClO_4)^-\cdot(psd)_2$. The electronic structure of ligand psd, in particular the bond order of Se−N bonds, has been probed by X-ray diffraction, ^{77}Se NMR, and computational studies. A detailed analysis of the crystal structures of the ligand and the complexes revealed interesting supramolecular assembly. The assembly was further facilitated by the presence of neutral ligands for some complexes (Cu(II) and Co(II)). The molecular structure of the ligand showed that it was present as a dimer in the solid state where the monomers were linked by strong secondary bonding Se···N interactions. The crystal structures of Cu(I) and Ag(I) complexes revealed the dinuclear nature with characteristic metallophilic interactions [M···M] (M = Cu, Ag), while the Cu(II) and Co(II) complexes were mononuclear. The presence of M···M interactions has been further probed by Atoms in Molecules (AIM) calculations. The paramagnetic Cu(II) and Co(II) complexes have been characterized by UV−vis, ESI spectroscopy, and room temperature magnetic measurements.

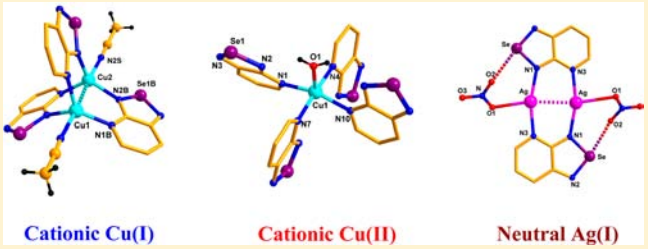

INTRODUCTION

Heavier chalcogens and halogens are known to display short interatomic contacts either between them or with the elements of other groups.[1] More recently such kinds of contacts have been attributed to secondary bonding interactions (SBIs) that are attractive in nature and have both orbital and electrostatic contributions.[2] All four 1,2,5-chalcogenadiazoles (**1**−**4**)[2,3] have been a favorite case-study to understand SBIs and the formation of supramolecular association through these SBIs (Figure 1a). The strength of electrostatic interaction between the negative nitrogen and the positive chalcogen atoms is guided by the electronegativity difference between them, which is highest in the case of Te. The electronic origin of secondary interaction between two chalcogenadiazole moieties is due to the donation of electron density from the lone pair of nitrogen to the antibonding E−N σ^* orbital of another chalcogenadiazole moiety (Figure 1b). Interestingly, apart from neutral chalcogenadiazoles, their cationic counterparts can too exhibit secondary E···N interactions.[4,5] The upsurge in the interest of such interactions involving heavier chalcogens is due to the fact that they are often instrumental in the construction of large supramolecular structures.

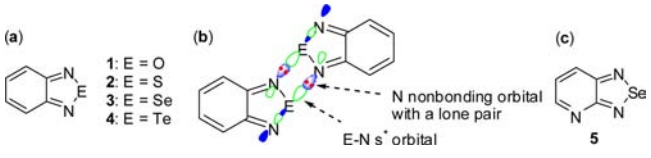

Figure 1. 1,2,5-Chalcogenadiazoles (**1**−**5**) shown in (**a**) and (**c**). Directional bonding between two chalcogenadiazoles by a nitrogen nonbonded orbital with a lone pair and an antibonding orbital of the E−N bond is shown in (**b**).

Two 1,2,5-selenadiazole rings can associate themselves through antiparallel Se···N SBIs to form a four-membered cyclic supramolecular synthon. This synthon can repeat itself to link another molecule, thus, giving a ribbon like polymer. It is interesting to note that the association of the chalcogenadiazoles can be controlled by suitable coordination of the nitrogen atom. For instance, the 1:1 triphenylborane adduct of 1,2,5-telluradiazolobenzene exists as a dimer, whereas the 2:1 adduct is monomeric.[6] The phenyl rings of the 2:1 adduct block the access of the nitrogen atoms from the second molecule to

Received: March 10, 2012
Published: July 17, 2012

   dx.doi.org/10.1021/ic3005272 | *Inorg. Chem.* 2012, 51, 8128−8140

tellurium, which in turn prevents the formation of a dimer. Benzo-1,2,5-telluradiazole,[2,7] 1,2,5-telluradiazole,[2,7] and phenanthro[9,10-C]-1,2,5-telluradiazole[8] form ribbon polymers, while 4,6-di-tert-butyl- and 4,6-dibromo-benzo-1,2,5-telluradiazole only form dimers through the formation of $[Te\cdots N]_2$ supramolecular synthon.[2,9] Recently, Vargas-Baca and co-workers reported the two thermochromic [α(yellow) and β(red)] packing polymorphs of 4,5,6,7-tetrafluorobenzo-1,2,5-telluradiazole and a pyridine coordinated telluradiazole. The α phase is metastable; at 127 °C the material undergoes an exothermic irreversible transition to the red polymorph. A third phase is also yellow and transforms into the red phase after the loss of solvent. In the crystal structures, the molecules are also associated through $[Te\cdots N]_2$ supramolecular synthon forming ribbon polymers and dimers, respectively.[10]

In 1984 Kaim has reported the carbonyl substitution reactions of $M(CO)_6$ (M = Cr, Mo, W) with the radical anions of ligands **1**, **2**, and **3**, which result in the replacement of CO and the formation of mononuclear paramagnetic complexes at first and then get converted to binuclear paramagnetic complexes.[11] Subsequently, the mononuclear Ni,[12] Co,[13] Cu,[14] Zn,[15] Hg,[16] Ru,[17,18] Os,[17] and Ir[17] complexes based on the ligands **2** and **3** were reported. The first report bearing Se···N SBIs for the construction of periodic supramolecular architectures reported was by Tong and co-workers.[19] It has been demonstrated that the silver(I) complex of 1,2,5-benzeneselenadiazole (bsd), along with neutral bsd leads to the formation of two polymorphs of silver(I) bsd complexes (α and β-$[Ag(bsd)_2(NO_3)]\cdot 0.5bsd$) with interesting three-dimensional supramolecular networks through Se···N interactions. Also, it has been shown that the use of **3** as an auxiliary ligand to construct the two-dimensional hexagonal honeycomb networks of Ag(I) ion in the crystal structures of $[Ag_3(btc)(bsd)_6]\cdot 0.5H_2O$ and $[Ag_3(ctc)(bsd)_3]\cdot 1.5bsd\cdot 3.5H_2O$ where btc =1,3,5-benzenetricarboxylate and ctc =1,3,5-cyclohexanetricarboxylate.[20] We envisaged that the introduction of one more nitrogen atom in the bsd ring (i.e., 1,2,5-selenadiazolopyridine, psd shown in Figure 1**c**) should lead to more interesting assemblies due to additional $Se\cdots N_{py}$ interactions. Since nitrogen based bidentate ligands with one carbon linker are capable of binding to two metal centers, it can also be used to synthesize metal complexes with closed shell metal···metal interactions. Reviews on such types of metal···metal interactions have been published by Leznoff et al. in 2008[21] and more recently by Sculfort and Braunstein.[22] The ligands of type NCN,[23] PCP, PNP, SCS,[24] PCN,[25] and OCO[25c] show metallophilic interactions when coordinated with d^{10} metal ions. With these ideas, we have chosen psd (**5**) as our ligand of choice for the study. The ligand has similar coordination sites i.e. NCN type and metallophilic interactions are expected despite the presence of an extra selenium atom which can play a part in the formation of supramolecular assemblies. Herein, we report the synthesis and characterization of **5** and its complexes with Cu(I), Ag(I), Cu(II), and Co(II). The nature of the short metal···metal distances in these complexes is further probed by theoretical studies.

EXPERIMENTAL SECTION

Materials and Procedures. Solvents were dried and distilled by standard procedures. 2,3-Diaminopyridine, selenium dioxide, tetrakis(acetonitrile)copper(I) hexafluorophosphate, copper(II) perchlorate hexahydrate, and cobalt(II) perchlorate hexahydrate were purchased from Aldrich. Silver nitrate and cupric nitrate were purchased from Sisco Research Laboratories, India. Silver trifluoroacetate,[26] tetrakis(acetonitrile)copper(I) perchlorate,[27] and tetrakis(acetonitrile)copper(I) chloride[28] were prepared according to literature procedures. ***Caution!*** *Perchlorate salts are potentially explosive. Although no detonation tendencies have been observed, caution is advised and handling of only small quantities is recommended.*

General Physical Measurements. Melting points were recorded in capillary tubes and are uncorrected. The ^1H, ^{13}C, and ^{77}Se NMR spectra were recorded on a Varian VXR 400 or VXR 300 spectrometer. Chemical shifts cited were referenced to TMS (^1H, ^{13}C) as internal and Me_2Se (^{77}Se) as external standard. Electron spray mass spectra (ESI-MS) were performed on a Q-Tof micro (YA-105) mass spectrometer. Mass spectra were obtained with a Platform II single quadrupole mass spectrometer (Micromass, Altrincham, UK) using a CH_3OH mobile phase. Elemental analyses were performed on a Carlo-Erba model 1106 elemental analyzer. IR spectra were recorded as KBr pellets on a Nicolet Impact 400 and Perkin FT-IR spectrometer. All UV−vis spectra and reflectance spectra were recorded on a Jasco-570 spectrophotometer. Reflectance spectra were recorded by using $BaSO_4$ as standard. Emission spectra were recorded by using a Perkin-Elmer LS55 luminescence spectrometer. Cyclic voltammetric measurements were carried out using a CH 1600 model electrochemistry system. A platinum wire working electrode, platinum wire auxiliary electrode, and saturated calomel reference electrode were used in a standard three-electrode configuration. Tetraethylammonium perchlorate was the supporting electrolyte, the scan rate used was 50 mV s^{-1}, and ferrocene was used as the standard. All of the electrochemical experiments were carried out under a nitrogen atmosphere, and all of the redox potentials are uncorrected for junction potentials. The ESR measurements were made with a Varian model 109CE-line X-band spectrometer fitted with a quartz Dewar for measurements at 77 K. ESR has been studied at room temperature as well as at liquid nitrogen temperature. TCNQ was taken as the standard. Magnetic susceptibility was measured on a PAR vibrating sample magnetometer.

Preparation of 1,2,5-Selenadiazolopyridine (5).[29] 2,3-Diaminopyridine (1.23 g, 11.27 mmol) and selenium dioxide (1.25 g, 11.27 mmol) were ground using a porcelain mortar and pestle at room temperature for 30 min. The crude black colored mixture obtained was extracted with benzene and filtered. The filtrate was concentrated under vacuum to get a yellow residue. The residue obtained was again dissolved in a mixture of acetone and ether (1:1 v/v) as a solvent, a pinch of charcoal was added, and the mixture was filtered. The solvent was concentrated under vacuum to obtain **5** as a pale yellow solid (1.55 g, 75% yield). Mp 118−120 °C (lit. mp 116−118 °C). FT-IR (KBr) 3049, 1590, 1504, 1485, 1375, 1208, 781; UV−visible, λ_{max} 335 nm (ε: 1.42×10^7 cm^2 mol^{-1}); ^1H NMR (400 MHz, $CDCl_3$) δ 8.99 (dd, J = 3.7, 1.6 Hz, 1H), 8.10 (dd, J = 8.8, 1.5 Hz, 1H), 7.32 (dd, J = 9.2, 4.0 Hz, 1H); ^{13}C NMR (400 MHz, $CDCl_3$) δ 164.5, 156.9, 153.4, 131.5, 123.8; ^{77}Se NMR (300 MHz, $CDCl_3$) δ 1476; ES-MS m/z (relative intensity, nature of peak) 186 (100, $[M+1]^+$); Anal. Calcd. for $C_5H_3N_3Se$: C, 32.63; H 1.64; N 22.83. Found C, 32.56; H, 1.29; N 23.07.

Synthesis of $[Cu_2(psd)_3(CH_3CN)_2](PF_6)_2$ (6). To a 50 mL two-necked flask was taken an acetonitrile solution (15 mL) of **5** (0.30 g, 1.63 mmol). To it was added an acetonitrile solution (2 mL) of $[Cu(CH_3CN)_4]PF_6$ (0.30 g, 0.81 mmol). The mixture was stirred for 1 h to obtain a brown-colored solution, and then the excess acetonitrile was removed by using vacuum. The precipitate obtained was recrystallized from acetonitrile (0.38 g, 90% yield). Mp 220−223 °C. FT-IR (KBr) 3550, 3414, 3236, 1637, 1617, 1519, 1019, 838, 767 cm^{-1}; UV−visible, λ_{max} 335 nm (ε: 6.06×10^4 cm^2 mol^{-1}), λ_{max} 507 nm (ε: 2.26×10^3 cm^2 mol^{-1}); ^1H NMR (400 MHz, DMSO-d_6) δ 9.09 (br, 3H), 8.33 (d, J = 8.7 Hz, 3H), 7.57 (br, 3H); ^{77}Se NMR (300 MHz, CD_3CN) δ 1492; ES-MS m/z (relative intensity, nature of peak) 247 (40, $[Cu(psd)]^+$); 433 (20, $[Cu(psd)_2]^+$); Anal. Calcd. for $C_{19}H_{15}Cu_2F_{12}N_{11}P_2Se_3$: C, 21.71; N, 14.66; H, 1.44. Found C, 21.82; N, 14.25; H, 0.82.

Synthesis of $[Cu_2(Cl)_2(psd)_3]$ (7). An acetonitrile solution of $CuCl(CH_3CN)_4$ (0.26 g, 1.00 mmol) was prepared *in situ* by dissolving CuCl (0.10 g, 1 mmol) in 10 mL of acetonitrile in a 25 mL

dx.doi.org/10.1021/ic3005272 | Inorg. Chem. 2012, 51, 8128−8140

one-necked flask.[28] To it was added a chloroform solution (5 mL) of **5** (0.28 g, 1.50 mmol). The mixture was stirred for 1 h to obtain a black-colored precipitate. The precipitate obtained was recrystallized from acetonitrile to give rectangular shaped crystals of **7** (0.21 g, 60% yield). Mp 141 °C. FT-IR (KBr) 1593 ($\upsilon_{C=N}$), 1529 ($\upsilon_{C=C}$) cm^{-1}; UV−visible, λ_{max} 336 nm (ligand) (ε: 7.50 × 10^4 cm^2 mol^{-1}). ES-MS *m*/*z* (relative intensity, nature of peak) 750 (17, $[M]^+$); 715 (18, $[M+H-Cl]^+$); 615 (20, $[M-CuCl-Cl]^+$); 530 (55, $[M-psd-Cl]^+$); 432 (50, $[M-psd-CuCl-Cl]^+$); 345 (60, $[M-2psd-Cl]^+$); 185 (100, $[M-2psd-2CuCl]^+$); Anal. Calcd. for $C_{15}H_9Cl_2Cu_2N_9Se_3$: C, 24.02; N, 16.80; H, 1.21. Found C, 24.26; N, 16.08; H, 1.61.

Synthesis of $[Cu(psd)_3](ClO_4)$ (8). To a 50 mL two-necked flask was taken an acetonitrile solution (7 mL) of **5** (0.28 g, 1.50 mmol). To it was added an acetonitrile solution (5 mL) of $[Cu(CH_3CN)_4]ClO_4$ (0.16 g, 0.51 mmol). The mixture was stirred for 1 h to obtain a brown-colored solution, and then the excess of acetonitrile was removed by using vacuum. The precipitate obtained was recrystallized from acetonitrile to give **8** (0.23 g, 63% yield). Mp 208−210 °C. FT-IR (KBr) 3441, 3071, 1590, 1510, 1379, 1296, 1223, 1088, 777, 621 cm^{-1}; UV−visible, λ_{max} 335 nm (ε: 8.04 × 10^4 cm^2 mol^{-1}); ^{1}H NMR (400 MHz, $CDCl_3$) δ 9.11 (br, 1H), 8.22−8.19 (m, 1H), 7.44−7.41 (m, 1H); ES-MS *m*/*z* (relative intensity, nature of peak) 185 (100, $[psd+H]^+$); 345 (5, $[Cu(psd)ClO_4+H]^+$); 432 (8, $[Cu(psd)_2+2H]^+$); 530 (5, $[Cu(psd)_2ClO_4+H]^+$); Anal. Calcd. for $C_{15}H_9ClCuN_9O_4Se_3$: C, 25.19; N, 17.63; H, 1.27. Found C, 25.66; N, 17.83; H, 1.12.

Synthesis of $[Ag_2(psd)_2](NO_3)_2$ (9). To an acetonitrile solution (2 mL) of $AgNO_3$ (0.35 g, 2.06 mmol) was added dropwise an acetonitrile solution (10 mL) of **5** (0.38 g, 2.06 mmol), and the reaction mixture was stirred further for 30 min. The precipitate obtained was filtered, washed with acetonitrile, and dried under vacuum. Recrystallization from acetonitrile/water (2:1) gave golden yellow prismatic crystals of **9** (0.67 g, 92% yield). Mp > 272 °C. FT-IR (KBr) 1587, 1515, 1385, 1135, 1020, 773 cm^{-1}; ^{1}H NMR (400 MHz, DMSO-d_6) δ 9.09 (dd, *J* = 4.2, 1.9 Hz, 2H), 8.40 (dd, *J* = 7.7, 1.8 Hz, 2H), 7.61 (dd, *J* = 7.7, 3.7 Hz), 2H); ^{13}C NMR (400 MHz, DMSO-d_6) δ 163.1, 157.7, 152.6, 132.4, 124.3; ^{77}Se NMR (300 MHz, DMSO-d_6) 1498; UV−visible, λ_{max} 336 nm (ε: 5.37 × 10^4 cm^2 mol^{-1}); ES-MS *m*/*z* (relative intensity, nature of peak) 292 (100, $[M\text{-}NO_3]^+$), 477 (5, $[Ag(psd)_2]^+$); Anal. Calcd. for $C_{10}H_6N_8O_6Se_2Ag_2$: C, 16.97; N, 15.83; H, 0.85. Found C, 17.08; N, 15.75; H, 0.59.

Synthesis of $[Ag_2(psd)_2](CF_3OCO)_2$ (10). To a 50 mL round-bottomed flask containing a solution of $Ag(CF_3OCO)$ (0.32 g, 1.47 mmol) in 2 mL of acetonitrile was added a 10 mL acetonitrile solution of **5** (0.27 g, 1.47 mmol). A deep yellow-colored precipitate appeared immediately. The mixture was further stirred for 30 min and filtered. The precipitate obtained was dried under vacuum and recrystallized from acetonitrile or acetonitrile/water (2:1) mixture to give orange plate shaped crystals of **10** (0.47 g, 81% yield). Mp 257−260 °C. FT-IR (KBr) 1683, 1587, 1208, 1136, 773, 724 cm^{-1}; ^{1}H NMR (400 MHz, DMSO-d_6) δ 9.08 (dd, *J* = 4.1, 1.8 Hz, 2H), 8.36 (dd, *J* = 8.7, 1.4 Hz, 2H), 7.59 (dd, *J* = 8.7, 3.6 Hz, 1H); ^{13}C NMR (400 MHz, DMSO-d_6) δ 161.3, 159.4, 159.0, 158.9, 152.4, 133.5, 124.5; ^{19}F NMR (300 MHz, CD_3CN) δ −74.7; ^{77}Se NMR (300 MHz, DMSO-d_6) δ 1502; UV−visible, λ_{max} 337 nm (ε: 8.51 × 10^3 cm^2 mol^{-1}); ES-MS *m*/*z* (relative intensity, nature of peak) 292 (100, $[M-C_2F_3O_2]^+$), 477 (95, $[Ag(psd)_2]^+$); Anal. Calcd. for $C_{14}H_6N_6O_4Se_2F_6Ag_2$: C, 20.76; N, 10.38; H, 0.75. Found C, 20.69; N, 10.43; H, 0.57.

Synthesis of $[Cu(psd)_2(H_2O)_3](ClO_4)_2\cdot(psd)_2$ (11). To a solution of $Cu(ClO_4)_2\cdot 6H_2O$ (0.18 g, 0.50 mmol) in 10 mL of methanol was added a 10 mL solution of **5** (0.37 g, 2.00 mmol) in the same solvent. The reaction mixture was stirred at room temperature for 1 h to afford a green solid, which was recrystallized from methanol to give green crystals of **11** (0.35, 66% yield). Mp 205 °C. FT-IR (KBr) 3419, 1590, 1526, 1505, 1373, 1130, 1145, 1089, 770, 626 cm^{-1}; UV−visible, λ_{max} 334 nm (ε: 2.19 × 10^6 cm^2 mol^{-1}); ES-MS *m*/*z* (relative intensity, nature of peak) 185 (100, $[psd+H]^+$); 247 (12, $[Cu(psd)]^+$); 432 (38, $[Cu(psd)_2]^+$); 531 (10, $[Cu(psd)_2+ClO_4]^+$); Anal. Calcd. for $C_{20}H_{18}Cl_2CuN_{12}O_{11}Se_4$: C, 22.82; N, 15.97; H, 1.72. Found C, 22.59; N, 15.88; H, 1.14.

Synthesis of $[Cu(psd)_4(H_2O)](ClO_4)_2\cdot CHCl_3$ (12). To a solution of $Cu(ClO_4)_2\cdot 6H_2O$ (0.18 g, 0.50 mmol) in 3 mL of chloroform was added a 5 mL solution of **5** (0.37 g, 2.00 mmol) in the same solvent. The reaction mixture was stirred at room temperature for 1 h to afford a green solid of **11**, which was removed by filtration. The resulting solution was further stirred at room temperature for 16 h and afforded a magenta-colored precipitate of **12** which was recrystallized from a 1:1 mixture of $CHCl_3$−MeOH to give violet colored crystals of **12** (0.36 g, 63% yield). Mp 267 °C (dec). FT-IR (KBr) 3456, 3049, 1590, 1525, 1505, 1374, 1298, 1211, 1142, 1089, 763, 625 cm^{-1}; UV−visible, λ_{max} 334 nm (ε: 7.80 × 10^4 cm^2 mol^{-1}); ES-MS *m*/*z* (relative intensity, nature of peak) 523 (5, $[Cu_2(psd)_2+MeO-3H]^+$); 370 (12, $[2psd+H]^+$); 253 (50, $[Cu(psd)+6H]^+$); 218 (100, $[psd+CH_3OH+2H]^+$); 185 (32, $[psd+H]^+$); Anal. Calcd. for $C_{21}H_{15}Cl_5CuN_{12}O_9Se_4$: C, 22.20; N, 14.79; H, 1.33. Found C, 22.27; N, 14.66; H, 1.05.

Synthesis of $Cu(psd)_2(H_2O)_3(NO_3)_2\cdot(H_2O)\cdot(psd)_2$ (13). To a 10 mL acetonitrile/water (v/v 3:1) solution of **5** (0.49 g, 2.67 mmol) was added an acetonitrile/water (6 mL, v/v 3:1) solution of copper nitrate trihydrate (0.32 g, 1.33 mmol), and then the mixture was stirred for 30 min to give a clear solution. A deep green precipitate was obtained on stirring for 2 days. The precipitate obtained was recrystallized from an acetonitrile/water solvent mixture to give green colored crystals of **13** (0.36, 32% yield). Mp 155−158 °C. FT-IR (KBr) 3444, 1590, 1526, 1511, 1384, 1312, 1296, 1220, 768 cm^{-1}; UV−visible, λ_{max} 335 nm (ε: 5.59 × 10^4 cm^2 mol^{-1}), λ_{max} 786 nm (ε: 34.66 cm^2 mol^{-1}); ES-MS *m*/*z* (relative intensity, nature of peak) 185 (100, $[psd]^+$); 433 (20, $[Cu(psd)_2]^+$); Anal. Calcd. for $C_{20}H_{20}CuN_{14}O_{10}Se_4$: C, 24.12; N, 19.69; H, 2.02. Found C, 24.20; N, 20.46; H, 1.43.

Synthesis of $[Co(psd)_2(H_2O)_4](ClO_4)_2\cdot(psd)_2$ (14). To a 5 mL methanol solution of **5** (0.19 g, 1.07 mmol) was added a methanol (5 mL) solution of cobalt perchlorate hexahydrate (0.11 g, 0.28 mmol), and then the mixture was stirred for 12 h to give a clear solution. The solution was allowed to slowly evaporate at room temperature to afford orange rectangular crystals of **14** (0.24, 88% yield). These crystals slowly become opaque over time. Mp 223−224 °C. FT-IR (KBr) 3189, 1650, 1592, 1505, 1174, 1090, 774, 627 cm^{-1}; ES-MS *m*/*z* (relative intensity, nature of peak) 185 (30, $[psd]^+$); 215 (20, $[psd+MeO]^+$); 306 (100, $[Co(psd)+2OMe]^+$); 429 (15, $[Co(psd)_2]^+$); 463 (20, $[Co(psd)_2+OH+H_2O]^+$); 528 (50, $[Co(psd)_2+ClO_4]^+$); UV−visible, λ_{max} 335 nm (ligand) (ε: 1.79 × 10^5 cm^2 mol^{-1}); ^{77}Se NMR (400 MHz, DMSO-d_6) δ 1507 (broad); Anal. Calcd. for $C_{20}H_{20}Cl_2CoN_{12}O_{12}Se_4$: C, 22.53; H, 1.89. Found C, 22.96; H, 1.81. μ_{eff}: 4.88 μ_B.

X-ray Crystallography. The diffraction measurements for compounds **5**, **9**, **12**, **13**, and **14** were performed on an Oxford diffraction Gemini diffractometer, and X-ray data for compound **6**, **7**, **8**, **10**, and **11** were collected on a Bruker Apex 2 diffractometer with graphite-monochromated Mo Kα radiation (λ = 0.7107 Å). The structures were solved by direct methods and full matrix least-squares refinement on F^2 (program SHELXL-97).[30] Hydrogen atoms were localized by geometrical means. A riding model was chosen for refinement. The isotropic thermal parameters of the H atoms were fixed at 1.5 times (CH_3 groups) or 1.2 times U_{eq} (Ar−H) of the corresponding C atom. Three ligands in complexes **6** and **7** and the chloride atom in **7** are disordered. The ligand occupancies refined to values of 0.730(2)/0.270(2); 0.858(2):0.142(2); and 0.744(3)/0.256(3) for **6**, 0.897(2)/0.103(2) for ligand of **7**, and 0.898(4)/0.102(4) for chloride ion of **7**. For **7**, one ligand lies on a symmetry element and thus has an occupancy of exactly 0.5. The CF_3 groups in **10** were refined with occupancy factors of 0.648(14)/0.352(14) and 0.738(9)/0.262(9). The perchlorate anions in complexes **12** and **14** are disordered and refined with occupancy factors of 0.539(9)/0.461(9) and 0.573(9)/0.427(9), respectively. In complex **13**, the water molecule and nitrate anion are disordered and were refined with occupancy factors 0.541(9)/0.459(9) for water molecule and 0.565(6)/0.435(6) and 0.579(8)/0.421(8) for nitrate anion.

Theoretical Calculations. DFT calculations were carried out using the Gaussian 03 suite of programs.[31] Atoms in molecules (AIM) analysis[32] was carried on the crystal geometry using the AIM 2000 program.[33] The wave functions for AIM analysis were generated by

dx.doi.org/10.1021/ic3005272 | *Inorg. Chem.* 2012, 51, 8128−8140

Scheme 1. Synthesis of Cu(I) Complexes

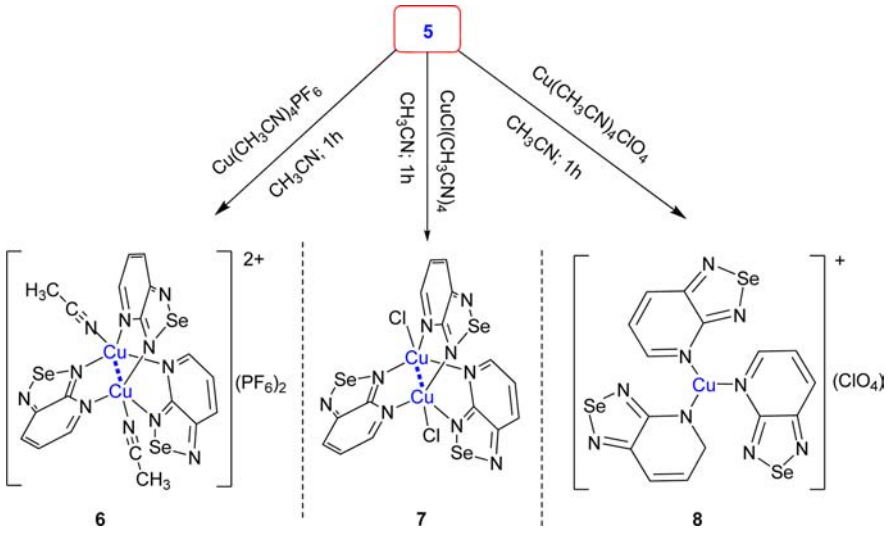

Scheme 2. Synthesis of Ag(I) Complexes

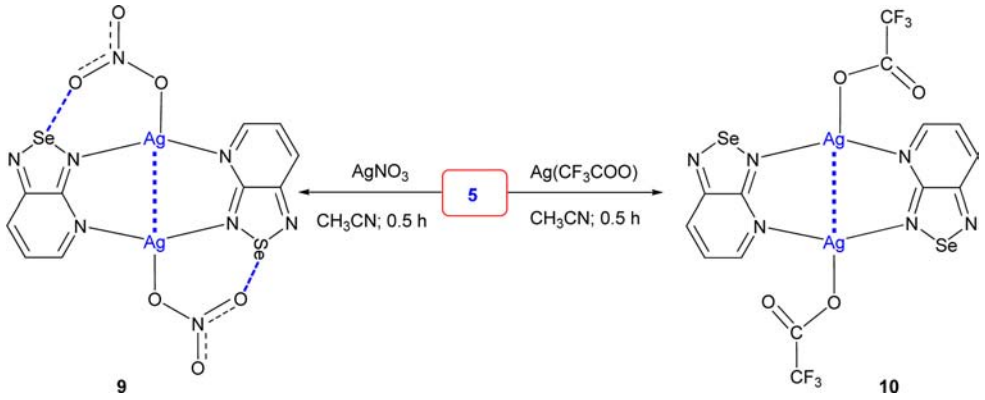

B3LYP using the WTBS basis set for Ag and Cu and 6-31 g(d) for the rest of the atoms.

RESULTS AND DISCUSSION

Synthesis. Selenadiazolopyridine **5** was prepared by the solid-state synthesis from 2,3-diaminopyridine and SeO_2 in 76% yield.[29] The reactions of Cu(I) and Ag(I) salts with **5** afforded $[Cu_2(psd)_3(CH_3CN)_2]^{2+}$ $2(PF_6)^-$ (**6**); $[(CuCl)_2(psd)_3]$ (**7**); $[Cu_2(psd)_6]^{2+}$ $2(ClO_4)^-$ (**8**); $[Ag_2(psd)_2]^{2+}$ $2(NO_3)^-$ (**9**); and $[Ag_2(psd)_2]^{2+}$ $2(CF_3COO)^-$ (**10**). Complexes **6**, **7**, and **8**, were synthesized by the reaction of **5** with $Cu(CH_3CN)_4PF_6$, $CuCl(CH_3CN)_4$, and $Cu(CH_3CN)_4ClO_4$, respectively (Scheme 1). The silver complexes $[Ag(psd)NO_3]$ (**9**) and $[Ag(psd)CF_3COO]$ (**10**) of selenadiazolopyridine were prepared by the treatment of **5** with corresponding silver salts in a 1:1 molar ratio in acetonitrile at room temperature (Scheme 2). All the complexes were obtained in high yields (>75%) and are soluble in common organic solvents and found to be air stable. In the Cu(I) and Ag(I) complexes, the ligand metal ions ratios are 3:1 and 1:1, respectively, and these ratios were also confirmed by elemental analysis and X-ray structure determination. (*vide infra*). The ES-MS spectra of these complexes did not show the molecular ion peaks, except for **7** (750 M^+) and ligand **5** (186 M^+). Two intense peaks seen at 433 and 247 for all the Cu(I) complexes were assigned to $[Cu(psd)_2]^+$ and $[Cu(psd)]^+$ ions, respectively. In addition, the other prominent peaks observed for complex **8** at 530 and 345 were assigned to $[Cu(psd)_2ClO_4+H]^+$ and $[Cu(psd)ClO_4+H]^+$ ions, respectively. Similarly complex **7** also shows four additional peaks at 715, 615, 530, and 345 assigned to $[M+H-Cl]^+$, $[M-CuCl-Cl]^+$, $[M-psd-Cl]^+$, and $[M-2psd-Cl]^+$, respectively. For Ag(I) complexes, peaks due to $[Ag(psd)_2]^+$ and $[Ag(psd)]^+$ were observed at 477 and 292, respectively.

Copper(II) complexes **11**, **12**, and **13** with selenadiazolopyridine were synthesized by the reaction of **5** with $[Cu(H_2O)_6](ClO_4)_2$ and $Cu(NO_3)_2{\cdot}3H_2O$, respectively (Scheme 3). The orange-colored Co(II) complex **14** was prepared similarly by the use of $[Co(H_2O)_6](ClO_4)_2$ (Scheme 3). The Cu(II) complexes are green in color, monomeric, and also soluble in common organic solvents such as acetonitrile, acetone, and dimethylsulfoxide. In the Cu(II) and Co(II) complexes, the ligand metal ions ratio is 4:1 where two ligands are coordinated to metal ions and the other two are present as neutral ligands except for **12** where all four ligands are coordinated to the metal ion. These aspects were confirmed by elemental analysis and X-ray structure determination. The ES-MS spectra of Cu(II) complexes show a similar trend to that observed for the Cu(I) complexes. The Co(II) complex **14** shows five prominent peaks at 528, 463, 429, 306, and 215 for $[psd+MeO]^+$, $[Co(psd)+2OMe]^+$, $[Co(psd)_2]^+$, $[Co(psd)_2+OH+H_2O]^+$, and $[Co(psd)_2+ClO_4]^+$) ions, respectively (Figure

dx.doi.org/10.1021/ic3005272 | *Inorg. Chem.* 2012, 51, 8128–8140

Scheme 3. Synthesis of Cu(II) and Co(II) Complexes

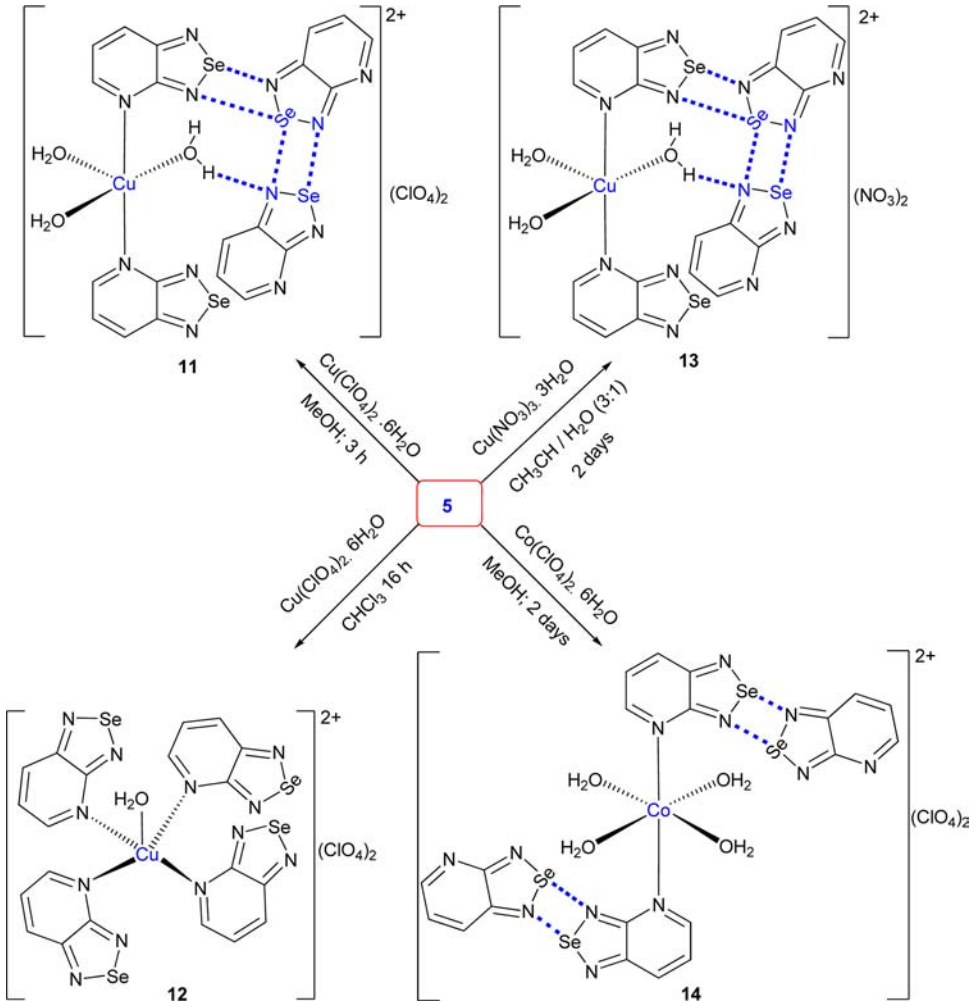

S7 in the ESI). From these data it is evident that the metal···ligand bond dissociates under ES-MS conditions.

Spectroscopic Studies. The complexes were characterized by FT-IR, ^{1}H, ^{13}C, and ^{77}Se spectroscopy. The ^{77}Se NMR spectrum of **5** exhibited a peak at 1477 ppm (Figure S3 in the ESI). The ^{1}H NMR spectrum of Cu(I) complexes showed three peaks in the aromatic region corresponding to three types of aromatic protons; however, the peaks were relatively broad. For the silver complexes, there was a very small shift of ^{1}H and ^{13}C signals as compared to that of free ligand **5**. The ^{19}F NMR spectrum of **10** showed a peak for the fluoro group at −74.7 ppm (Figure S4 in the ESI). The ^{77}Se NMR spectrum of **10** exhibited a peak at 1498 ppm (Figure S5 in the ESI), whereas for **9** it was observed at 1502 ppm (Figure S6 in the ESI). This downfield shift in the ^{77}Se NMR as compared to **5** (1476 ppm) can be attributed to the loss of electron density in the psd ring due to coordination of the nitrogens with the metal ion. The small downfield shift indicates no coordination of selenium with the metal ions. Though the ^{77}Se NMR chemical shift is in the range reported for coordination with Se(II) to Cu(I), the structure determination does not show any coordination in this case (*vide infra*).[34]

The electronic spectra of the ligand and the complexes were recorded in solution and in the solid state. The solution phase electronic spectra of the ligand as well as all the complexes show an intense band at ∼335 nm. This ligand based transition at 335 nm can be assigned as $\pi-\pi^*$ transition which was further confirmed by TD-DFT calculations.[35] Compound **6** shows an additional weak and broad band at 507 nm which may be due to the metal to ligand charge-transfer (MLCT transition). In the solid state it gives a broad peak at ∼548 nm (Table S2 in the ESI). The room temperature electronic spectrum of Cu(II) complex **13** in methanol exhibits a very weak transition at ∼786 nm which can be assigned to a d-d (t_{2g}-e_g) band.[35] The UV−vis spectrum of **9** in the solid state showed a band at 407 nm, whereas for **10** it appeared at 393 nm and corresponds to a ligand based transition. The silver complexes were found to be luminescent in the solid state. The solid-state emission spectrum of **9** and **10** exhibited peaks at 480 and 525 nm when excited at 407 and 393 nm, respectively (Figures S8 and S9 in the ESI). These emission bands are ligand based emissions, which also appear in the emission spectrum of selenadiazolopyridine. However, the intensity of these fluorescence peaks of the complexes is greater than that observed for the ligand.

The ESR spectrum of the Cu(II) complexes were recorded at 77 K in a methanol−acetone (4:1) mixture and DMSO solvent. The analysis of spectra shows $g_{II(av)}$ at 2.30−2.48 with $A_{(av)}$ 166 and 185 G and $g_{\perp(av)}$ at 2.07 (Table 1). The higher value of $g_{II(av)}$ as compared to $g_{\perp(av)}$ indicates a $d_{x^2-y^2}$ ground state for the **12** and **13** complexes. The trend $g_{\|} > 2.1 > g_{\perp}$ observed for the Cu(II) complexes indicates that the unpaired electron is

dx.doi.org/10.1021/ic3005272 | *Inorg. Chem.* 2012, 51, 8128−8140

Table 1. EPR Parameters of Cu(II) 12, 13, and Co(II) 14 Complexes

complex	g	10^{-4} A (cm^{-10})
12 in MeOH−actone (4:1)	$g_{\|\|}$ 2.48; $g_{\perp}$ 2.07	$A_{\|\|}$ 185.44
13 in DMSO	$g_{\|\|}$ 2.30; $g_{\perp}$ 2.07	$A_{\|\|}$ 166.39
14 in DMSO	g_1 2.17; g_2 2.11; g_3 2.04;	A_1 89.75; A_2 96.71; A_3 86.28;
	g_4 1.98; g_5 1.90; g_6 1.86	A_4 94.33; A_5 88.28

localized in the $d_{x^2-y^2}$ orbital of the Cu(II) ion, and spectral features are characteristic of axial symmetry. The $g_{\|\|}$ and $A_{\|\|}$ values are strongly affected by the ligand environment in a tetragonal Cu(II) site.[36] The higher $g_{\|\|}$ value of **12** compared to **13** suggest the presence of strong axial interaction. The EPR spectra of Co(II) complex were recorded as a polycrystalline sample and in DMSO solutions at liquid nitrogen temperature. The 'g' values were found to be almost the same in both cases. This indicates that the complexes have the same geometry in solid form as well as in the solution. Additionally, complexes **12**−**14** exhibit superhyperfine structure in the $g_{\perp}$ region.

The room-temperature magnetic moment of the complex **13** was found to be μ_{eff} (299.2 K) = 2.12 μ_B which is higher than expected for spin only magnetic moment for the d^9 system. Such a value is typical of magnetically dilute complexes and may result from the contribution of excited state orbital angular momentum.[37] The magnetic moment of the complex **14** was found to be μ_{eff} (299.2 K) = 4.88 μ_B corresponding to three unpaired electrons as expected for high-spin Co(II) in an octahedral environment.

The cyclic voltammetric experiments of the complexes **6**−**13** were recorded at 0.5 mM concentration using tetrabutylammonium perchlorate as supporting electrolyte. Since complex **6** exists as a dinuclear copper(I) unit, the two Cu^I units are oxidized to form dinuclear Cu(II) at 0.665 V (Figure S10 in the ESI). However, when the cycle is reversed one of the Cu(II) is reduced to Cu(I) at 0.509 V and results in the formation of a mixed valence Cu(I)−Cu(II) system. The other Cu(I) center reduces at 0.258 V to give back the dinuclear Cu(I) complex. Complex **8** shows only the oxidation peak at 0.0336 V indicating the decomposition of the complex in the solution under redox conditions (Figure S11 in the ESI). In the cyclic voltammetry experiment, Cu(II) complex **13** showed two irreversible redox peaks (E_{pc} −0.309 V and E_{pa} −0.025) (Figure S12 in the ESI). The rest of the Cu(I) **7** and Cu(II) **11** and **12** complexes did not show any oxidation reduction peak. Cyclic voltammogram of Ag(I) complexes **9** and **10** showed reduction peaks at −0.211 and 0.0242 V, respectively. When the scan was reversed, the oxidation peaks occurred at 0.072 V and −0.246 V, respectively (Figures S13 and S14 in the ESI). The reduction reaction of Ag^+ is $Ag^+ + 1e^- \rightarrow Ag$. Silver ion in the solution takes one electron and becomes Ag and after that the oxidation reaction $Ag \rightarrow Ag^+ + 1e^-$ occurs where the silver atom loses an electron to become the Ag^+ ion. The ΔE_p = ∼245 mV for both the copper (**6** and **13**) and silver complexes (**9** and **10**) indicating the redox process is irreversible.

Solid-State Structure Analysis. Crystal data and structure refinement details for **5**−**14** are given in Tables 2 and 3. The molecular structure of **5** is shown in Figure 2a. Ligand **5** crystallizes in a monoclinic crystal system with the $P2_1/c$ space group. In solid state, the pyridine ring of the molecule exhibits a quinoid type of structure. The C5A−N2A and C1A−N1A bond lengths are 1.318(6) Å and 1.329(6) Å, respectively, and thus have a double bond character. The C5A−C1A bond, which is common to the five- and six-membered rings of **5**, has a bond length of 1.454(6) Å. This bond distance represents an exclusive single bond and is longer than that observed for selenadiazolobenzene, where it has a value of 1.437(9) Å.[3c] However in **4**, the corresponding distance is longer and has values of 1.658(10) and 1.475(9) Å in the two asymmetric units.[2a] The two psd rings are associated by two antiparallel

Table 2. Crystallographic Data and Refinement Details for 5, 6, 7, 8, 9, and 10

compound	**5**	**6**	**7**	**8**	**9**	**10**
empirical formula	$C_5H_3N_3Se$	$C_{43}H_{35}Cu_4F_{24}N_{25}OP_4Se_7$	$C_{15}H_9Cl_2Cu_2N_9Se_3$	$C_{15}H_9ClCuN_9O_4Se_3$	$C_{10}H_6Ag_2N_8O_6Se$	$C_{28}H_{12}Ag_4F_{12}N_{12}O_8Se_4$
formula weight	184.06	2304.72	750.17	715.18	707.89	1619.82
crystal system	monoclinic	orthorhombic	monoclinic	monoclinic	monoclinic	triclinic
space group	$P2_1/c$	$Pbca$	$C2/c$	$C2/c$	$P2_1/a$	P-1
a (Å)	11.2836(8)	11.823(3)	17.964(2)	21.297(4)	7.0106(3)	7.870(4)
b (Å)	8.3584(5)	24.824(6)	9.3797(9)	13.268(3)	11.4083(3)	10.539(5)
c (Å)	12.7110(8)	48.413(11)	12.7632(17)	14.070(3)	10.3530(3)	12.227(6)
α (deg)	90	90	90	90	90	94.575(16)
β (deg)	111.156(8)	90	112.678(70)	96.189(12)	91.257(3)	93.754(18)
γ (deg)	90	90	90	90	90	102.847(16)
V (Å^3)	1118.01(14)	14209(6)	1984.3(4)	3952.7(14)	827.82(5)	982.0(8)
Z	8	8	4	8	2	1
D(calcd) (Mg/m^3)	2.187	2.155	2.511	2.404	2.840	2.739
T (K)	173(2)	293(2)	100(2)	173(2)	173(2)	173(2)
range of θ (deg)	4.8 to 32.5	1.64 to 21.11	2.75 to 30.04	2.91 to 25.25	4.99 to 32.52	2.48 to 28.55
abs coeff (mm^{-1})	6.603	4.977	7.942	6.815	6.816	5.797
obsd reflens [$I > 2\sigma$]	3569	7620	2825	3553	2768	4638
final R_1 [$I > 2\sigma(I)$]	0.0509	0.0961	0.0614	0.0541	0.0295	0.0425
wR_2 indices [$I > 2\sigma$]	0.1051	0.2224	0.1270	0.1194	0.0552	0.0861
data/restraints/parameters	3569/0/163	7620/1284/1067	2825/197/178	3553/0/298	2768/0/127	4638/84/364
goodness of fit on F^2	1.131	0.975	1.139	0.979	0.896	1.074

dx.doi.org/10.1021/ic3005272 | Inorg. Chem. 2012, 51, 8128−8140

Table 3. Crystallographic Data and Refinement Details for 11, 12, 13, and 14

compound	11	12	13	14
empirical formula	$C_{20}H_{18}Cl_2Cu$ $N_{12}O_{11}Se_4$	$C_{21}H_{15}Cl_5Cu$ $N_{12}O_9Se_4$	$C_{20}H_{20}Cu$ $N_{14}O_{10}Se_4$	$C_{30}H_{26}Cl_2Co$ $N_{18}O_{12}Se_6$
formula weight	1052.74	1136.08	995.88	1434.28
crystal system	triclinic	monoclinic	triclinic	triclinic
space group	*P*-1	$P2_1/c$	*P*-1	*P*-1
a (Å)	11.2674(7)	17.2767(7)	11.4192(3)	8.5454(3)
b (Å)	11.4607(8)	11.5563(3)	14.1808(5)	11.7953(5)
c (Å)	13.3644(8)	18.8398(6)	20.6650(6)	11.8973(5)
α (deg)	100.188(4)	90	79.063(3)	78.854(4)
β (deg)	96.877(7)	114.083(4)	74.977(2)	74.315(4)
γ (deg)	106.360(3)	90	86.968(2)	81.414(3)
V (Å^3)	1603.31(18)	3434.0(2)	3173.23(17)	1126.77(8)
Z	2	4	2	1
D(calcd) (Mg/m^3)	2.181	2.197	2.143	2.114
T (K)	173(2)	173(2)	200(2)	295(2)
range of θ(deg)	3.09 to 30.86	3.22 to 30.11	4.6 to 32.5	5.10 to 35.96
abs coeff (mm^{-1})	5.465	5.333	5.352	5.425
obsd reflens [$I > 2\sigma$]	9578	8173	19932	9176
final R_1 [$I > 2\sigma(I)$]	0.0338	0.0454	0.0742	0.0533
wR_2 indices [$I > 2\sigma$]	0.0664	0.0975	0.1962	0.1023
data/restraints/parameters	9578/9/469	8173/43/468	19932/283/917	9176/78/363
goodness of fit on F^2	1.010	1.078	1.188	1.009

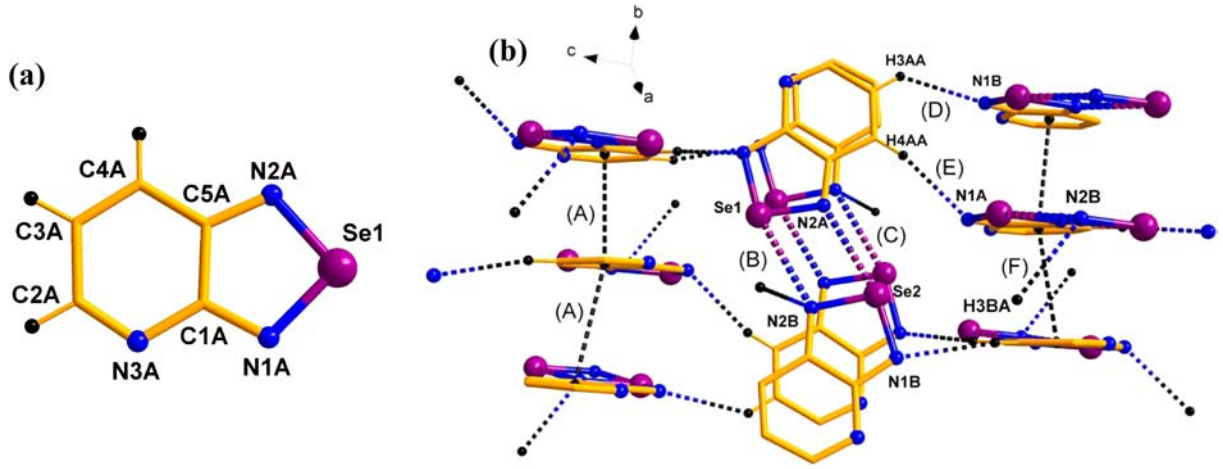

Figure 2. Molecular structure of the **5** (**a**) and 3-D supramolecular motif *via* $\pi\cdots\pi$, Se···N SBIs, and C−H···N hydrogen bonding in the lattices of **5** (**b**). Selected bond distances [Å] and angles [°]: molecule A (molecule B); Se−N(1) 1.781(5) (1.780(6)), Se−N(2) 1.792(4) (1.793(4)), (A) = 3.601(0), (B) = 2.956(5), (C) = 2.888(5), (D) 2.632(4), (E) = 2.537(5), (F) = 2.568(4); N(1)−Se−N(2) 94.41(19) (94.40(19)). Only relevant hydrogen atoms are shown for clarity.

Se···N SBIs forming a four-membered cyclic supramolecular synthon. The intermolecular Se···N distances in this dimeric unit are 2.888(7) Å and 2.956(7) Å. These synthons are interconnected in the lattice via $\pi\cdots\pi$ interactions and C−H···N hydrogen bonding interactions (Figure 2b).

The structure of chalcogenadiazolopyridine can be represented by two Kekule structures (Figure 3), one having chalcogen atom, E as divalent (**I**) and the other structure having it as tetravalent (**II**).

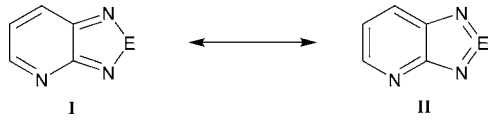

I **II**

Figure 3. Kekule structures of **5**.

Crystal Structures of Cu(I) Complexes 6, 7, and 8. The molecular structures of **6**, **7**, and **8** are shown in Figure 4a, 4b, and 4c, respectively. Complex **6** crystallizes in an orthorhombic crystal system with the *Pbca* space group, while **7** and **8** crystallize in a monoclinic system with the *C*2/*c* space group. The primary geometry around the Cu atoms of **6** and **7** is distorted trigonal bipyramidal (for **6**, τ values range from 0.78 to 0.51 with an average value of 0.68, while for **7**, τ is 0.69), while for **8** it is best described as trigonal planar but with a weak Cu···Se out of plane interaction. Distortion of molecular geometry in these complexes is caused by the steric demands of the ligands attached to the central atom. The copper atoms in complexes **6**, **7**, and **8** are coordinated through three nitrogen atoms from ligands, with acetonitrile and chloride ion coordinating axially in **6** and **7**, respectively. The core of the complexes **6** and **7** is propeller-shaped, and **8** has a fan shaped

dx.doi.org/10.1021/ic3005272 | *Inorg. Chem.* 2012, 51, 8128−8140

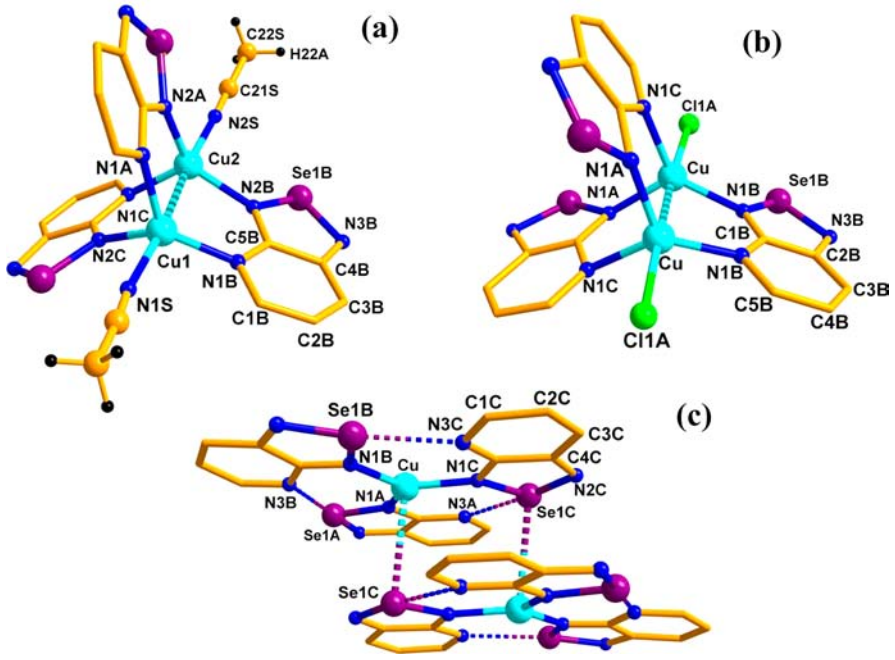

Figure 4. Molecular Structures of compounds **6** (**a**), **7** (**b**), and **8** (**c**). The PF_6^- (for **6**) and ClO_4^- (for **8**) anions along with the hydrogen atoms of aryl carbon frames are omitted. Only one set of atoms for the disordered Cl and psd in (**7**) is shown. Selected bond parameters are summarized in Table 4.

Table 4. Selected Bond Parameters for Compounds 6, 7, and 8

bond lengths [Å]		bond angles [deg]	
6			
Cu(1)−N(1A) 2.071(8)	Cu(1)−N(1B) 2.016(8)	N(1A)−Cu(1)−N(2C) 102.7(4)	N(1A)−Cu(1)−N(1B) 124.9(4)
Cu(1)−N(2C) 2.059(6)	Cu(2)−N(2A) 2.005(8)	N(1B)−Cu(1)−N(2C) 127.7(3)	N(1C)−Cu(2)−N(2A) 108.7(4)
Cu(2)−N(2B) 2.032(7)	Cu(2)−N(1C) 2.026(7)	N(1C)−Cu(2)−N(2B) 120.0(3)	N(2A)−Cu(2)−N(2B) 125.5(4)
Cu(1)−N(1S) 2.134(7)	Cu(2)−N(2S) 2.167(8)		
Cu(1)···Cu(2) 2.884(2)			
7			
Cu−N(1A) 2.054(5)	Cu−N(1B) 2.045(7)	N(1A)−Cu−N(1C) 104.4(14)	N(1A)−Cu−N(1B) 123.2(6)
Cu−N(1C) 2.158(49)	Cu−Cl(1A) 2.488(2)	N(1B)−Cu−N(1C) 129.4(16)	
Cu···Cu 2.860(1)			
8			
Cu−N(1A) 1.979(7)	Cu−N(1B) 1.982(7)	N(1A)−Cu−N(1B) 120.2(3)	N(1A)−Cu−N(1C) 118.6(3)
Cu−(1C) 1.987(8)	Cu···Se(1C) 3.160(2)	N(1B) −Cu−N(1C) 120.8(3)	N(2A)−Se(1A)···N(3B) 179.7(3)
Se(1A)···N(3B) 2.714(9)	Se(1B)···N(3C) 2.711(8)	N(2B)−Se(1B)···N(3C) 174.0(3)	N(2C)−Se(1C)···N(3A) 175.8(3)
Se(1C)···N(3A) 2.697(7)			

structure with the ligands. The ligands are acting as the blades of the propeller and fan. The crystal structures revealed a unique feature *i.e.* the presence of Cu···Cu [2.869(2) and 2.860(1) Å] metallophilic interactions in **6**, **7**, and Cu···Se [3.160(2) Å], metal···metalloid interactions in **8**, which is longer than most of the complexes which exhibit Cu(I)···Cu(I) interactions[38] and is shorter than Σ r_{vdw} of Cu···Cu (4.0 Å) and Cu···Se(3.9).[39] For **8**, where the coordination environment about the Cu is trigonal planar, the ligands are arranged so that there are interatomic Se···N(pyridine) distances which range from 2.697(7) Å to 2.714(9) Å. These are longer than Σ r_{cov} (Se,N), 1.90 Å, but significantly shorter than Σ r_{vdw} (Se,N), 3.45 Å indicating the presence of attractive intramolecular 1,6-Se···N secondary bonding interactions. In spite of possible rotation about the Cu−N bonds, the ligands in **8** are oriented so that the selenium and nitrogen atoms of pyridine rings and copper atom are almost in the equatorial plane. Coplanarity, together with near linearity of the N···Se−N(*trans*) triad(s) (N···Se−N ∼ 176.5°), make n→σ^* orbital interaction; therefore, it appears to be the major component of the attractive interaction between the lone pair of hypervalent Se and N atoms (Figure 4c). Among the crystal lattices of these complexes, C−H···O and C−H···X interactions are thus the only associative forces that give rise to supramolecular motifs *via* self-assembly (Supporting Information, Figures S15 and S16).

Selected bond parameters for **6**, **7**, and **8** are summarized in Table 4.

Crystal Structures of Ag(I) Complexes 9 and 10. The molecular structures and supramolecular assemblies of **9** and **10** are given in Figure 5. Complex $[Ag(psd)NO_3]_2$ **9** crystallizes in a monoclinic crystal system with the $P2_1/a$ space group. The asymmetric unit consists of four formula units, and, therefore, there are four crystallographically unique (but chemically

dx.doi.org/10.1021/ic3005272 | *Inorg. Chem.* 2012, 51, 8128−8140

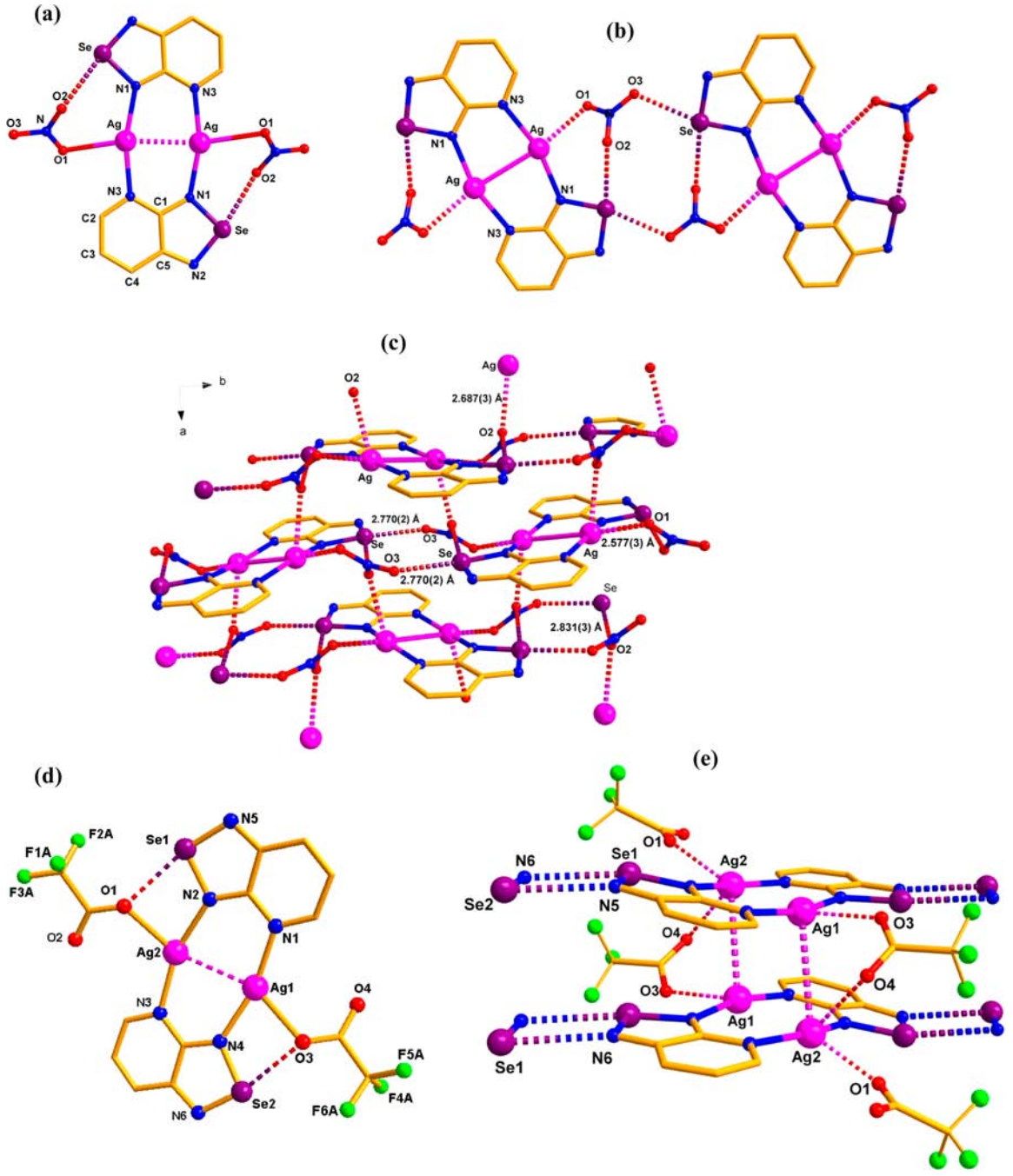

Figure 5. Molecular units for complexes **9** and **10** are shown in (**a**) and (**d**). The assembly into a two-dimensional ladder type network for **9** is shown in (**b**) and (**c**), while (**e**) shows the supramolecular motif and intermolecular Se···N interactions in **10** leading to one-dimensional network. Only one set of atoms for the disordered CF_3 groups is shown. The hydrogen atoms of aryl carbon frames are omitted for clarity.

similar) silver atoms, four unique psd ligands, and four nitrate ions. Complex **9** has a dinuclear structure with an almost planar eight-membered metallacycle ring. Selenadiazolopyridine acts as a bridging bidentate ligand as it is bonded to two silver atoms through its nitrogen atoms (N1, N3, N1#, N3#). The Ag–N bond distances are Ag–N1 2.206(3) Å and Ag–N3 2.204(3) Å and are less than the Σr_{cov} (Ag,N), 2.27 Å. The silver atom is coordinated by the two psd ligands almost linearly, and the N–Ag–N# bond angle is 161.4°. The N1–Ag–Ag#–N3 and N1–Ag–Ag#–N1# dihedral angles are 180.0° and 9.69°, respectively.

One of the important features of the complex is the relatively short Ag···Ag distance (2.931(0) Å) in the eight-membered metallacycle ring. This distance of 2.931 Å is shorter than Σr_{vdw} of Ag–Ag 3.54 Å.[38] The intramolecular Ag···Ag separation in **9** is longer than Ag···Ag distances in $[Ag_2(p\text{-}CH_3C_6H_4NCHNC_6H_4\text{-}p\text{-}CH_3)_2]$ (2.705(1) Å),[40] $[Ag_2L(\mu\text{-}ONO_2)](NO_3)\cdot 2H_2O$ (2.901 Å; L = 1,4-bis(2-hexahydropyrimidyl)benzene),[41] and $[Ag_2L_2](ClO_4)_2\cdot CH_3CN$ (2.776(1) Å; L = 4,5-diazospirobifluorene)[42] but shorter than $[Ag_2(Ph_2PCH_2PPh_2)_2](NO_3)_2$ (3.085(1) Å).[43] This short distance between the silver atoms may be a consequence of

dx.doi.org/10.1021/ic3005272 | Inorg. Chem. 2012, 51, 8128–8140

Table 5. Selected Bond Parameters for Compounds 9 and 10

bond lengths [Å]		bond angles [deg]	
9			
Ag–N(1) 2.206(3)	Ag–N(3) 2.204(3)	N(1) –Ag–N(3) 161.46(10)	N(1)–Ag–Ag 80.92(7)
Ag–O(1) 2.577(3)	Ag···Ag 2.931(0)	N(1)–Ag–O(1) 109.11(9)	N(3)–Ag–Ag 83.25(7)
Se···O(2) 2.831(3)		N(3)–Ag–O(1) 87.68(10)	
10			
Ag(1)–N(1) 2.160(4)	Ag(1)–N(4) 2.201(4)	N(1)–Ag(1)–N(4) 164.98(15)	N(1)–Ag(1)–Ag(2) 88.37(11)
Ag(2)–N(2) 2.245(4)	Ag(2)–N(3) 2.186(4)	N(4)–Ag(1)–Ag(2) 78.55(10)	N(1)–Ag(1)–O(3) 114.01(16)
Ag(1)–O(3) 2.355(5)	Ag(2)–O(1) 2.328(4)	N(4)–Ag(1)–O(3) 77.82(15)	N(2)–Ag(2)–N(3) 158.89(15)
Ag(1)···Ag(2) 2.969(1)		N(2)–Ag(2)–Ag(1) 75.26(10)	N(3)–Ag(2)–Ag(1) 84.81(11)
		N(2)–Ag(2)–O(1) 75.89(14)	N(3)–Ag(2)–O(1) 119.06(15)

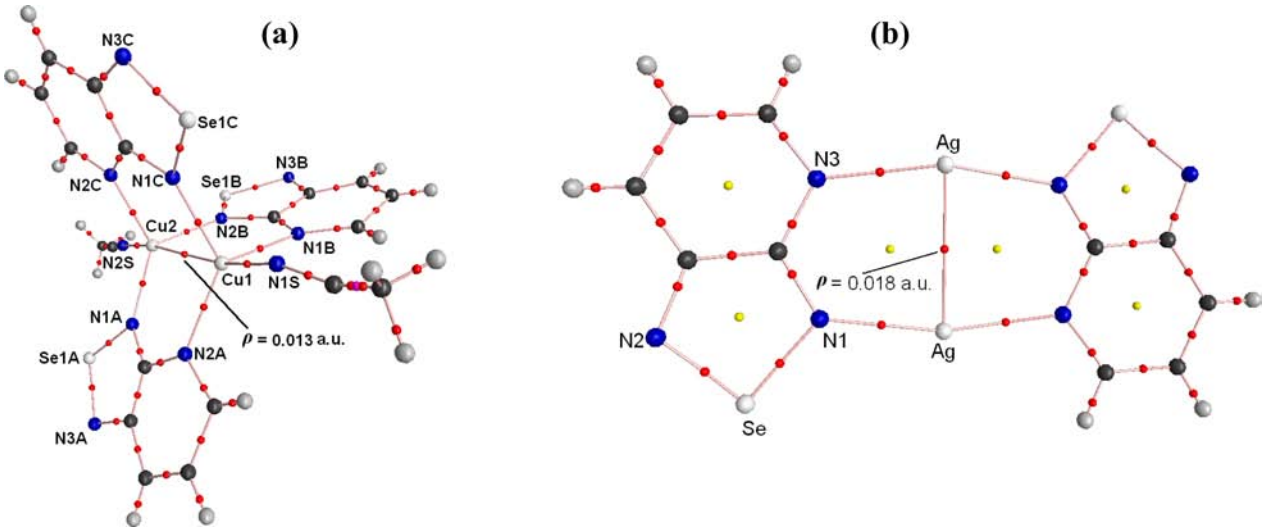

Figure 6. AIM pictures of **6** (**a**) and **9** (**b**) showing the presence of bond critical points between Cu···Cu and Ag···Ag atoms, respectively.

metallophilic interaction which in the case of silver is commonly known as an argentophilic interaction.

The nitrate group in the crystal acts as a bridging ligand to connect antiparallel binuclear $Ag_2(psd)_2(NO_3)_2$ units (Figure 5b) thus forming a two-dimensional ladder type chain network (Figure 5c). Apart from the Ag–O (nitrate) bond, two nitrate oxygen atoms are involved in intermolecular Se···O interactions, in which the distance between Se and O are 2.770 Å and 2.831 Å. In addition, there is a short intermolecular contact between selenium and nitrogen atoms between two antiparallel binuclear units, and this distance is 3.340 Å.

The single crystals of the complex **10** were isolated as orange plates from an acetonitrile and water solution (2:1) for the X-ray diffraction study. $[Ag(psd)(CF_3COO)]_2$ crystallizes in the triclinic crystal system with the *P*-1 space group. Complex **10** has similar structural features as that of the nitrate complex **9** which includes a binuclear structure with an almost planar eight-membered metallacycle ring (Figure 5c). In complex **10** also, psd acts as a bridging bidentate ligand and is bonded to two silver atoms through nitrogen atoms with Ag–N bond distances being Ag1–N1 2.161(4) Å, Ag1–N4 2.203(4) Å, Ag2–N2 2.253(4) Å, and Ag2–N3 2.191(4) Å. The N1–Ag1–Ag2–N3 torsion angle is 175.51(17)°, whereas the N1–Ag1–Ag2–N2 angle is 2.74(17)°. The N1–Ag1–N4 and N2–Ag2–N3 bond angles are deviated from linearity and have the values 165.09(17)° and 158.72(16)°, respectively. The Ag···Ag distance is longer than the distance observed in nitrate complex **9** and has the value 2.969 Å.

Interestingly, in complex **10**, the carboxylate group of trifluoroacetate acts as a bridge between two adjacent dinuclear $[Ag_2(psd)_2(CF_3COO)_2]$ units and leads to the formation of Ag_4 cluster. In this Ag_4 cluster, the Ag1 atom of one unit is at a distance of 3.521 Å and 3.327 Å from the Ag2 and Ag1 atom of the next unit of tetramer. The molecule can be expanded in one dimension via intermolecular Se···N interactions, the Se···N distances being 2.912 Å and 2.928 Å. These intermolecular Se···N interactions formed between two Ag_4 clusters is the first example of unique Ag_4 supramolecular assembly mediated by short Se···N interactions (Figure 5e).

Selected bond parameters for **9** and **10** are summarized in Table 5.

To investigate the presence of metal···metal interactions in complexes **6**, **9**, and **10**, we carried out Atoms in Molecules (AIM) analysis on their crystal geometries using the AIM2000 program. The cationic part of **9** was chosen for the analysis of Ag complexes, as both the complexes **9** and **10** have the same cation. The single point calculation on crystal geometry was performed by Gaussian 03 quantum chemical program. The AIM analysis involves topological properties of the electron density (ρ) to describe bonds among interacting atoms. Chemical bonding can be identified by the presence of a bond critical point (bcp), which is defined in AIM formalism as a point where electron density reaches a minimum along the bond path. For both the complexes **6** and **9**, the bond critical point exists between Cu···Cu (Figure 6a) and Ag···Ag (Figure 6b) which substantiates the metal···metal bonding in the

dx.doi.org/10.1021/ic3005272 | *Inorg. Chem.* 2012, 51, 8128–8140

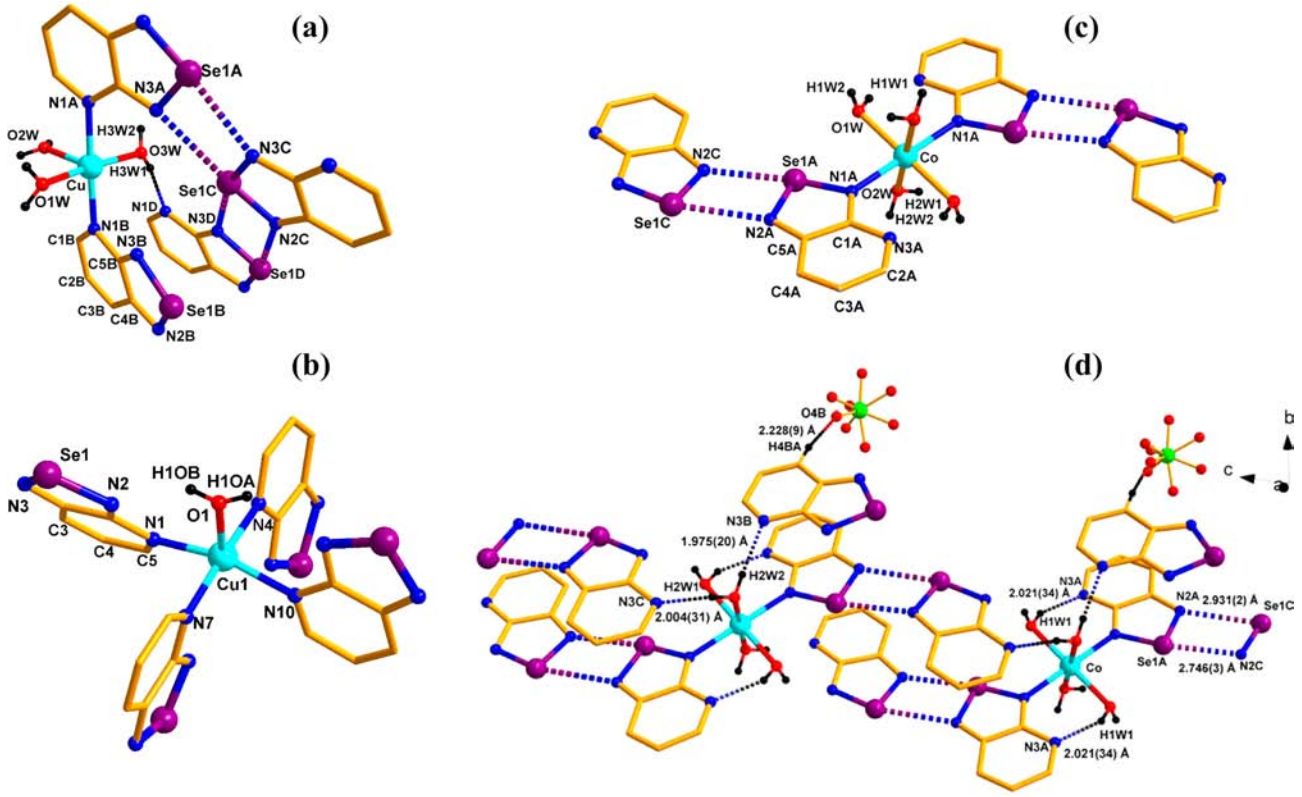

Figure 7. Molecular structures of compounds **11** (a), **12** (b), and **14** (c). The ClO_4^- (for **11**, **12**, and **14**) anions along with the hydrogen atoms of aryl carbon frames are omitted. A 2D supramolecular motif in crystal lattice of **14** (**d**) involving Se···N SBIs, C–H···F, and C–H···N hydrogen bonding interactions.

Table 6. Selected Bond Parameters for Compounds 11, 12, and 14

bond lengths [Å]		bond angles [deg]	
11			
Cu–N(1A) 2.015(3)	Cu–N(1B) 2.024(3)	O(1W)–Cu–O(2W) 96.93(9)	O(2W) –Cu–O(3W) 93.47(9)
Cu–O(1W) 1.949(2)	Cu–O(2W) 2.308(2)	O(1W)–Cu–O(3W) 169.60(9)	
Cu–O(3W) 1.946(2)	Se(1A)···N(3C) 2.834(2)		
Se(1C)···N(3A) 3.016(2)	Se(1C)···N(3D) 3.000(3)		
Se(1D)···N(2C) 2.871(3)	H(3W1)···N(1D) 1.962(33)		
12			
Cu(1)–N(1) 2.061(4)	Cu(1)–N(4) 2.011(5)	N(1)–Cu(1)–N(4) 90.77(15)	N(1)–Cu(1)–N(7) 88.60(15)
Cu(1)–N(7) 2.016(4)	Cu(1)–N(10) 2.092(3)	N(4)–Cu(1)–N(10) 89.36(15)	N(7)–Cu(1)–N(10) 89.17(15)
Cu(1)–O(1) 2.184(4)		N(1)–Cu(1)–O(1) 100.41(15)	N(4)–Cu(1)–O(1) 92.80(17)
		N(7)–Cu(1)–O(1) 92.46(16)	N(10)–Cu(1)–O(1) 102.70(15)
14			
Co–N(1A) 2.123(3)	Co–O(1W) 2.099(2)	N(1A)–Co–O(1W) 87.44(11)	N(1A)–Co–O(2W) 91.03(10)
Co–O(2W) 2.079(3)	Se(1A)···N(2C) 2.746(3)	O(1W)–Co–O(2W) 92.09(11)	O(2W)–Co–O(1W) 87.92(11)
Se(1C)···N(2A) 2.9306(2)		N(1A)–Co–O(2W) 88.97(10)	N(1A)–Co–O(1W) 92.56(11)

synthesized complexes. The value of ρ_{bcp} for Ag–Ag bcp (0.018 au) and Cu–Cu bcp (0.013 au) is much lower than a normal covalent bond but in the range of metal···metal bonds.[40] It has been observed that the total energy density ($H = G + V$), which is the sum of the electronic kinetic energy density (G) and the electronic potential energy density (V), is a more reliable parameter in ascertaining the nature of a chemical bond. Covalent interactions are characterized by a negative value of H, while ionic ones are characterized by positive values.[44] The positive values of H_{Ag-Ag} (0.0374 au) and H_{Cu-Cu} (0.0199 au) obtained for Ag···Ag and Cu···Cu interactions respectively indicate more contribution from the ionic character.

Crystal Structures of Cu(II) Complexes 11, 12, 13, and Co(II) Complex 14. These monomeric metal(II) complexes crystallize in the triclinic crystal system with space group $P\text{-}1$ except **14** which crystallizes in a monoclinic crystal system with the $P2_1/c$ space group. Molecular structures of Cu(II) (**11**, **12**) and Co(II) (**14**) complexes are shown in Figure 7a, 7b, and 7c, respectively.

The three Cu(II) complexes are all five-coordinate and all have a distorted square pyramidal structure (τ = 0.101, 0.298, and 0.217/0.242 for **11**, **12**, and **13**, respectively), while the Co(II) complex is six-coordinate. For the Cu(II) complexes the stoichiometry is different in that two have a $CuL_2(H_2O)_3$

dx.doi.org/10.1021/ic3005272 | Inorg. Chem. 2012, 51, 8128–8140

coordination sphere, while the third has a $CuL_4(H_2O)$ coordination sphere. This shows that even slight changes in synthetic conditions lead to complexes of different composition.

In complexes **11** and **13** the two psd ligands are in *trans* position, and two water molecules occupy the equatorial plane. The axial position is occupied by the third water molecule, while in complexes **12** the four psd ligands are occupied in an equatorial plane and one water molecule is occupied in an axial position. The Cu−N and equatorial Cu−O distances in Cu(II) complexes are in the range of 2.011(5) to 2.092(3) Å and 1.927(3) to 1.956(3) Å, respectively. In all three Cu(II) complexes, the axial Cu−O bonds are significantly longer [2.184(4) to 2.308(2) Å] than the equatorial Cu−O bonds indicating a weaker bonding. For **14**, the Co(II) atom sits on an inversion center with four water molecules in that equatorial plane and two psd ligands at the axial positions. The Co−N bond length 2.123(3) Å does not significantly differ from the average distances found for related Co(II) complexes.[13,45] The Co−O bond lengths [2.099(2), 2.079(3) Å] are close to the average distances reported for $[Co(H_2O)_4(adenine)_2]^{2+}$ ion.[45]

A search of the Cambridge structural database showed that Cu(II) complexes that have CuN_2O_3 coordination with three water molecules and two nitrogen atoms are relatively rare.[46] One recent example involves a guanine containing Cu(II) complex where the Cu−OH_2 bond distances (axial Cu−O: 2.298(3) Å; equatorial Cu−O: 1.950(3), 1.937(3) Å) are close to those found in **11**, **13**, and **14**.[47]

One of the important features of the solid structures of **11**, **13**, and **14** is the presence of two psd ligands which are not coordinated to the central atom. These free psd moieties are involved in intermolecular Se···N interaction which gives rise to a complex supramolecular assembly in **14** (Figure 7d).

Selected bond parameters are summarized in Table 6.

CONCLUSIONS

In conclusion, the presence of pyridine nitrogen in selenadiazolopyridine and its complexes leads to novel supramolecular association involving Se···N interactions. Ag(I) forms a dimeric or tetrameric complexes, whereas Cu(I) forms a dimeric complex bridged by three selenadiazolopyridine ligands. In the case of metal ions with closed shell configuration e.g (Ag(I), Cu(I)), the selenadiazolopyridine reinforces metallophilic interactions between the metal ions.

ASSOCIATED CONTENT

Supporting Information

X-ray crystallographic data for ligand **5** and complexes **6**−**14** in cif format, spectral data (^1H, ^{13}C, ^{77}Se NMR, emission spectra, and ES-MS) for selected complexes, CV of **6**, **8**, **9**, **10**, and **13**, elemental analysis, and ORTEP diagrams of all complexes. This material is available free of charge via the Internet at http://pubs.acs.org.

AUTHOR INFORMATION

Corresponding Author

*E-mail: chhbsia@chem.iitb.ac.in.

Notes

The authors declare no competing financial interest.

ACKNOWLEDGMENTS

H.B.S. is grateful to the Department of Science and Technology (DST), New Delhi, for funding. P.S. thanks Indian Institute of Technology, Bombay for a Post Doctoral Fellowship, and S.S. thanks UGC for a SRF.

REFERENCES

(1) (a) Bleiholder, C.; Werz, D. B.; Köppel, H.; Gleiter, R. *J. Am. Chem. Soc.* **2006**, *128*, 2666. and references therein. (b) Nakanishi, W.; Hayashi, S. *Chem.—Eur. J.* **2008**, *14*, 5645. (c) Lari, A.; Bleiholder, C.; Rominger, F.; Gleiter, R. *Eur. J. Inorg. Chem.* **2009**, 2765.

(2) (a) Cozzolino, A. F.; Britten, J. F.; Vargas-Baca, I. *Cryst. Growth Des.* **2006**, *6*, 181. (b) Cozzolino, A. F.; Vargas-Baca, I.; Mansour, S.; Mahmoudkhani, A. H. *J. Am. Chem. Soc.* **2005**, *127*, 3184.

(3) (a) Bailey, A. *J. Chem. Soc.* **1967**, 2107. (b) Bagryanskaya, I. Yu.; Gatilov, Yu. V.; Makarov, A. Yu.; Shakirov, M. M.; Shuvaev, K. V.; Zibarev, A. V. *Russ. J. Gen. Chem.* **2001**, *71* (7), 1055. (c) Gomes, S. E.; Biswas, G.; Banerjee, A.; Duax, W. L. *Acta Crystallogr., Sect. C: Cryst. Struct. Commun.* **1989**, *C45*, 73.

(4) Risto, M.; Reed, R. W.; Robertson, C. M.; Oilunkaniemi, R.; Laitinen, R. S.; Oakley, R. T. *Chem. Commun.* **2008**, 3278.

(5) Berionni, G.; Pégot, B.; Marrot, J.; Goumont, R. *Cryst. Eng. Comm.* **2009**, *11*, 986.

(6) Cozzolino, A. F.; Bain, A. D.; Hanhan, S.; Vargas-Baca, I. *Chem. Commun.* **2009**, 4043.

(7) Bertini, V.; Dapporto, P.; Lucchesini, F.; Sega, A.; Munno, A. D. *Acta Crystallogr., Sect. C: Cryst. Struct. Commun.* **1984**, *40*, 653.

(8) Neidlein, R.; Knecht, D.; Gieren, A.; Ruiz-Perez, C. *Z. Naturforsch., B: J. Chem. Sci.* **1987**, *42*, 84.

(9) Chivers, T.; Gao, X. L.; Parvez, M. *Inorg. Chem.* **1996**, *35*, 9.

(10) Cozzolino, A. F.; Whitfield, P. S.; Vargas-Baca, I. *J. Am. Chem. Soc.* **2010**, *132*, 17265.

(11) Kaim, W. *J. Organomet. Chem.* **1984**, *264*, 317.

(12) Barkigia, K. M.; Renner, M. W.; Senge, M. O.; Fajer, J. *J. Phys. Chem. B* **2004**, *108*, 2173.

(13) Papaefstathiou, G. P. S.; Perlepes, S. P.; Escuer, A.; Vicente, R.; Gantis, A.; Raptopoulou, C. P.; Tsohos, A.; Psycharis, V.; Terzis, A.; Bakalbassis, E. G. *J. Solid State Chem.* **2001**, *159*, 371.

(14) Fun, H.-K.; Goh, J. H.; Maity, A. C.; Goswami, S. *Acta Crystallogr., Sect. E: Struct. Rep. Online* **2011**, *E67*, m-181.

(15) Fun, H.-K.; Maity, A. C.; Maity, S.; Goswami, S.; Chantrapromma, S. *Acta Crystallogr., Sect. E: Struct. Rep. Online* **2008**, *E64*, m-1188.

(16) Milios, C. J.; Ioannou, P. V.; Raptopoulou, C. P.; Papaefstathiou, G. S. *Polyhedron* **2009**, *28*, 3199.

(17) Herberhold, M.; Hill, A. F. *J. Organomet. Chem.* **1989**, *377*, 151.

(18) Alcock, N. W.; Hill, A. F.; Roe, M. S. *J. Chem. Soc., Dalton Trans.* **1990**, 1737.

(19) Zhou, A.-J.; Zheng, S.-L.; Fang, Y.; Tong, M.-L. *Inorg. Chem.* **2005**, *44*, 4457.

(20) Tan, C.-K.; Wang, J.; Leng, J.-D.; Zheng, L.-L.; Tong, M.-L. *Eur. J. Inorg. Chem.* **2008**, 771.

(21) Katz, M. J.; Sakai, K.; Leznoff, D. B. *Chem. Soc. Rev.* **2008**, *37*, 1884.

(22) Sculfort, S.; Braunstein, P. *Chem. Soc. Rev.* **2011**, *40*, 2741.

(23) (a) Song, H.-B.; Zhang, Z.-Z.; Mak, T. C. W. *J. Chem. Soc., Dalton Trans.* **2002**, 1336. (b) Zhang, J.-F.; Fu, W.-F.; Gan, X.; Chen, J.-H. *Dalton Trans.* **2008**, 3093. (c) Mohamed, A. A.; Abdou, H. E.; Fackler, J. P., Jr. *Coord. Chem. Rev.* **2010**, *254*, 1253. (d) Melgarejo, D. Y.; Chiarella, G. M.; Fackler, J. P., Jr.; Perez, L. M.; Alexandre Rodrigue-Witchel, A.; Reber, C. *Inorg. Chem.* **2011**, *50*, 4238. (e) Melgarejo, D. Y.; Chiarella, G. M.; Fackler, J. P., Jr. *Organometallics* **2011**, *30*, 5374. (f) Caballero, A. B.; Maclaren, J. K.; Rodríguez-Diéguez, A.; Vidal, I.; Dobado, J. A.; Salas, J. M.; Janiak, C. *Dalton Trans.* **2011**, *40*, 11845.

(24) (a) He, X.; Yam, V. W.-W. *Coord. Chem. Rev.* **2011**, *2111*−*2123*, 255. (b) Laguna, A.; Laguna, M. *Coord. Chem. Rev.* **1999**, *193*−*195*, 837.

(25) (a) Kazushi Mashima, K.; Tanaka, M.; Tani, K. *Inorg. Chem.* **1996**, *35*, 5244. (b) Kuang, S.-M.; Zhang, Z.-Z.; Wang, Q.-G.; Mak, T. C. W. *Inorg. Chem.* **1998**, *37*, 6090. (c) Bachechi, F.; Burini, A.; Galassi, R.; Macchioni, A.; Pietroni, B. R.; Ziarelli, F.; Zanello, P.; Zuccaccia, C. *J. Organomet. Chem.* **2000**, *593*−*594*, 392. (d) Jalil, M. A.; Yamada, T.; Fujinami, S.; Honjo, T.; Nishikawa, H. *Polyhedron* **2001**, *20*, 627. (e) Bachechi, F.; Burini, A.; Fontani, M.; Galassi, R.; Macchioni, A.; Pietroni, B. R.; Zanello, P.; Zuccaccia, C. *Inorg. Chim. Acta* **2001**, *323*, 45. (f) Catalano, V. J.; Horner, S. J. *Inorg. Chem.* **2003**, *42*, 8430. (g) Bachechi, F.; Burini, A.; Galassi, R.; Pietroni, B. R.; Ricciutelli, M. *Inorg. Chim. Acta* **2004**, *357*, 4349. (h) Keen, A. L.; Doster, M.; Han, H.; Johnson, S. A. *Chem. Commun.* **2006**, 1221. (i) Gina, M.; Chiarella, G. M.; Melgarejo, D. Y.; Rozanski, A.; Hempte, P.; Perez, L. M.; Reberb, C.; Fackler, J. P., Jr. *Chem. Commun.* **2010**, *46*, 136. (j) Li, Y.-J.; Deng, Z.-Y.; Xu, X.-F.; Wu, H.-B.; Cao, Z.-X.; Wang, Q.-M. *Chem. Commun.* **2011**, *47*, 9179.

(26) Haszeldine, R. N. *J. Chem. Soc.* **1951**, 584.

(27) Hathaway, B. J.; Holah, D. G.; Postlethwaite, J. D. *J. Chem. Soc.* **1961**, 3215.

(28) Yanagihara, N.; Ogura, T. *Transition Met. Chem.* **1987**, *12*, 9.

(29) Brown, N. M. D.; Bladon, P. *Tetrahedron* **1968**, *24*, 6577.

(30) (a) Sheldrick, G. M. *SHELXS-97, Program for Crystal Structures Solution*; University of Göttingen: Göttingen, Germany, 1997. (b) Sheldrick, G. M. *SHELXL-97, Program for Crystal Structures Refinement*; University of Göttingen: Göttingen, Germany, 1997.

(31) Frisch, M. J. et al.. Gaussian 03, revision C.02; Gaussian, Inc.: Wallingford, CT, 2004.

(32) Bader, R. F. W. *Atoms in Molecules- A Quantum Theory*; Clarendon Press: Oxford, 1990.

(33) Biegler-König, F.; Schönbohm, J.; Bayles, D. *J. Comput. Chem.* **2001**, *22*, 545.

(34) (a) Black, J. R.; Levason, W. *J. Chem. Soc., Dalton Trans.* **1994**, 3225. (b) Levason, W.; Orchard, S. D.; Reid, G. *Coord. Chem. Rev.* **2002**, *225*, 159−199.

(35) TD-DFT calculations (at B3LYP/6-31G(d), SDD level; SDD basis set with corresponding pseudopotential was used for the metal atoms and 6-31G(d) for the remaining atoms including Se in gas phase on crystal geometry. The calculations were performed on some of the representative complexes and ligand to predict the nature of electronic transitions. TD-DFT analysis on ligand **5** showed an intense peak at 288 nm (f = 0.234) that corresponds to the experimental λ_{max} of 335 nm and is primarily a π-π^* transition (see the ESI). For compound **6**, TD-DFT analysis showed an intense peak at 296 nm (f = 0.138) corresponding to ligand based π-π^* transition and the peak at 549 nm (f = 0.04) due to MLCT (see the ESI), which are in agreement with experimental values. For complex **13**, the band at 786 nm in UV−visible spectrum was in good agreement with 761 nm obtained from TD-DFT analysis (761 nm, f = 0.0001, see the ESI) and is a metal based d-d transition.

(36) Lal, T. K.; Gupta, R.; Mahapatra, S.; Mukherjee, R. *Polyhedron* **1999**, *18*, 1743 and references theirein.

(37) (a) Earnshaw, A. *The Introduction to Magnetochemistry*; Academic Press: London; 1980; p 80. (b) Koh, L. L; Ranford, J. O.; Robinson, W. T.; Svensson, J. O.; Tan, A. L. C.; Wu, D. *Inorg. Chem.* **1996**, *35*, 6466.

(38) (a) Johnson, A. L.; Willcocks, A. M.; Richards, S. P. *Inorg. Chem.* **2009**, *48*, 8613. (b) Zhang, J.-P.; Wang, Y.-B.; Huang, X.-C.; Lin, Y.-Y.; Chen, X.-M. *Chem.—Eur. J.* **2005**, *11*, 552. (c) Flavello, L. R.; Urriolabetia, E. P.; Mukhopadhyay, U.; Ray, D. *Acta Crystallogr., Sect. C: Cryst. Struct. Commun.* **1999**, *C55*, 170. (d) Rios-Moreno, G.; Aguirre, G.; Parra-Hake, M.; Walsh, P. J. *Polyhedron* **2003**, *22*, 563. (e) Coyle, J. P.; Monillas, W. H.; Yap, G. P. A.; Barry, S. T. *Inorg. Chem.* **2008**, *47*, 683. (f) Li, Z.; Barry, S. T.; Gordon, R. G. *Inorg. Chem.* **2005**, *44*, 1728. (g) Lim, B. S.; Rahtu, A.; Park, J.-S.; Gordon, R. G. *Inorg. Chem.* **2003**, *42*, 7951.

(39) Batsanov, S. S. *Inorg. Mater.* **2001**, *37*, 871.

(40) Cotton, F. A.; Feng, X.; Matusz, M.; Poli, R. *J. Am. Chem. Soc.* **1988**, *110*, 7077.

(41) Ren, C.-X.; Ye, B.-H.; Zhu, H.-L.; Shi, J.-X.; Chen, X.-M. *Inorg. Chim. Acta* **2004**, *357*, 443.

(42) Wang, C.-C.; Yang, C.-H.; Tseng, S.-M.; Lin, S.-Y.; Wu, T.-Y.; F, M.-R.; Lee, G.-H.; Wong, K.-T.; Chen, R.-T.; Cheng, Y.-M.; Chou, P.-T. *Inorg. Chem.* **2008**, *43*, 4781.

(43) Bau, R.; Ho, D. M. *Inorg. Chem.* **1983**, *22*, 4073.

(44) Iwaoka, M.; Komatsu, H.; Katsuda, T.; Tomoda, S. *J. Am. Chem. Soc.* **2004**, *126*, 5309−5317.

(45) Meester, P. D.; Skapski, A. C. *J. Chem. Soc., Dalton Trans.* **1973**, 1596.

(46) (a) Du, M.; Bu, X. -H.; Huang, Z.; Chen, S.-T.; Guo, Y.-M.; Diaz, C.; Ribas, J. *Inorg. Chem.* **2003**, *42*, 552. (b) Yilmaz, V. T.; Andac, O.; Yazicilar, T. K.; Kutuk, H.; Bekdemir, Y.; Harrison, W. T. A. *J. Mol. Struct.* **2002**, *608*, 71.

(47) Mastropietro, T. F.; Armentao, D.; Grisolia, E.; Zanchini, C.; Lloret, F.; Julve, M.; Munno, G. D. *Dalton Trans.* **2008**, 514.